reaction are entirely consistent with the results of the dehydro silylation reactions discussed earlier.

Both the phosphine-substituted cluster $Ru_3(CO)_9(PPh_3)_3$ and the mononuclear complex $Ru(CO)_3(PPh_3)_2$ were also found to catalyze the reaction of 2,3-$Et_2C_2B_4H_6$ with 2-butyne; however, in contrast to the reaction with $Ru_3(CO)_{12}$, high selectivity for the insertion product II was observed. In both cases the formation of II was again accompanied by the production of approximately equivalent amounts of 2-butene.

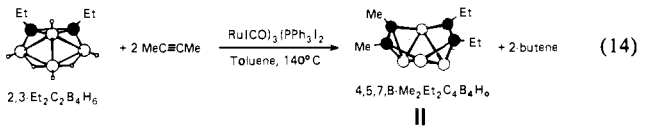

(14)

II

While the mechanism of reaction involving the ruthenium complexes has not yet been established, a reasonable sequence based on those proposed[34] for dehydro silylation reactions can be formulated, as outlined in Figure 3.[35] Thus, important initial steps probably involve (1) binding of the 2-butyne, (2) oxidative addition of the carborane, and (3) insertion of 2-butyne into a Ru–boron bond to form a (η^1-vinylcarborane)ruthenium species (D). If D then undergoes a β-hydride-elimination reaction involving the geminal methyl group, such as was proposed above for I, then formation of II would result. If, on the other hand, reductive elimination occurs, then the alkenylcarborane III would be formed. Thus, the degree of product selectivity should be dependent on the relative rates of β-hydride- and reductive-elimination reactions. Furthermore, the elimination reactions should be influenced by, for example, the electronic and steric properties of the other ligands present at the metal. Thus, the higher selectivity for the insertion product (II) observed with $Ru_3(CO)_9(PPh_3)_3$ and $Ru(CO)_3(PPh_3)_2$ rather than $Ru_3(CO)_{12}$ could result from the fact that phosphine ligands may destabilize Ru^0 intermediates, relative to carbon monoxide, and reduce the driving force for the reductive-elimination step.[36]

The above comments concerning the mechanism of the reactions with ruthenium complexes are, of course, entirely speculative, and the determination of the exact reaction sequence will require detailed studies; however, the similarity of dehydro silylation and dehydro alkyne insertion reactions seems clear. Furthermore, in both the iron and ruthenium systems important steps leading to insertion appear to involve β-hydride alkene elimination and intramolecular hydroboration steps. This conclusion suggests, for example, that other dehydrogenation or olefin isomerization catalysts should now be examined for dehydro alkyne insertion activity and that the development of general metal-catalyzed carbon insertion reactions based on these types of catalysts may be possible.

Acknowledgment. We thank the National Science Foundation for the support of this research. We also thank Dr. Don Berry for many useful discussions concerning this research.

Supplementary Material Available: Tables of anisotropic temperature factors, hydrogen atom coordinates, bond distances, bond angles, and least-squares planes (10 pages); listings of observed and calculated structure factor amplitudes (5 pages). Ordering information is given on any current masthead page.

(34) Seitz, F.; Wrighton, M. S. *Angew. Chem., Int. Ed. Engl.* **1988**, *27*, 289-291.

(35) This reaction sequence assumes that mononuclear ruthenium fragments are the catalytically active species. For $Ru_3(CO)_{12}$ and $Ru_3(CO)_9(PPh_3)_3$, this may not be true and either di- or trimetallic units may be involved in the reaction; however, steps similar to those presented in Figure 3 are still possible.

(36) Halpern, J. *Acc. Chem. Res.* **1982**, *15*, 332-338 and references therein.

Stepwise Dehydrogenation of a Ru(III) Hexaamine Cage Complex to a Hexaimine Ru(II) Complex via Ru(IV) Intermediates

Paul Bernhard* and Alan M. Sargeson*

Contribution from the Research School of Chemistry, The Australian National University, G.P.O. Box 4, Canberra 2601, Australia. *Received March 28, 1988*

Abstract: The sexidentate ligand sarcophagine (sar: 3,6,10,13,16,19-hexaazabicyclo[6.6.6]eicosane) when coordinated to ruthenium(III) (**1**) rapidly undergoes oxidative dehydrogenation to introduce an imine group into the cap portion of the ligand. Successive two-electron oxidations lead to a stable Ru(II) hexaimine complex, with all the imine groups in the cage caps. Each of the imine groups stabilizes the Ru(II) state by ~0.15 V leading to a stability of the Ru(II) hexaimine complex which is comparable to that of $Ru(2,2'\text{-bipyridine})_3^{2+}$. $Ru(sar)^{3+}$ disproportionates in aqueous solution to $Ru^{II}sar^{2+}$ and a singly deprotonated Ru(IV) intermediate (λ_{max} (ϵ_{max}): 445 nm (7800 M^{-1} cm^{-1})) which is converted into the Ru(II) imine product by both a base- and an acid-catalyzed pathway. Intermediate di- and triimine complexes were also observed en route to the hexaimine species. The kinetic and thermodynamic data for the disproportionation process imply that the secondary nitrogen in $Ru(sar)^{3+}$ is quite acidic (pK_a: 5-6) and that the Ru(IV) state is stabilized by ≥2 V. Acid catalysis of the dehydrogenation process from $[Ru^{IV}sar\text{-}H]^{3+}$ as well as a reversible hydration of $Ru(imsar)^{2+}$ below pH 2.5 are interpreted in terms of protonation at the metal center.

The reactivity of amine ligands coordinated to ruthenium, in particular their oxidation to imines and nitriles, has been the focus of a number of studies[1,2] sparked by the general interest in metal ion catalysis of such oxidation processes and the photochemical properties of Ru(II) complexes with unsaturated N ligands. Due to the stability of encapsulated metal complexes[3] in general, it was thought that the Ru(II)/(III) complexes of such ligands and

(1) (a) Lane, B. C.; Lester, J. E.; Basolo, F. *J. Chem. Soc., Chem. Commun.* **1971**, 1618. (b) Mahoney, D. F.; Beattle, J. K. *Inorg. Chem.* **1973**, *12*, 2561. (c) Diamond, S. E.; Tom, G. M.; Taube, H. *J. Am. Chem. Soc.* **1975**, *97*, 2661. (d) Brown, G. M.; Weaver, T. R.; Keene, F. R.; Meyer, T. J. *Inorg. Chem.* **1976**, *15*, 190. (e) Adcock, P. A.; Keene, F. R.; Smythe, R. S.; Snow, M. R. *Inorg. Chem.* **1984**, *23*, 2336.

(2) (a) Ridd, M. J.; Keene, F. R. *J. Am. Chem. Soc.* **1981**, *103*, 5733. (b) Keene, F. R.; Ridd, M. J.; Snow, M. R. *J. Am. Chem. Soc.* **1983**, *105*, 7075 and references therein.

(3) Sargeson, A. M. *Pure Appl. Chem.* **1984**, *56*, 1603 and references therein.

0002-7863/89/1511-0597$01.50/0

especially the unsaturated variety would give interesting redox and photochemical properties, and we have begun to explore their synthesis and reactivity.

Attempts to synthesize Ru cage complexes from $Ru(en)_3^{3+}$ (en: 1,2-ethanediamine) by the usual template strategy were unsuccessful, presumably because the intermediate imine species, greatly stabilized by Ru(II), were not reactive enough toward nucleophilic attack. We have, however, recently synthesized the complex $Ru(sar)^{2+}$ (**1**) (sar = 3,6,10,13,16,19-hexaazabicyclo[6.6.6]eicosane) by a different route employing the remarkably labile $[Ru(N,N'\text{-dimethylformamide})_6]^{2+}$ complex.[4] This route has now been used successfully with other cage and cage-related ligands.

It has been argued that the Ru(IV) oxidation state plays an important role in the facile oxidation of coordinated amines. Evidence supporting these arguments can be documented readily.[1,2] $[(NH_3)_5Ru(pyridine)]^{3+}$ was found to disproportionate to the Ru(II) and Ru(IV) ions in basic media.[5] In the related Ru-oxo systems Ru(IV) compounds have been isolated[6] and used as two-electron oxidizing agents.[7] Similarly, the result of a recent kinetic study[2] on the dehydrogenation of the $[(bpy)_2Ru(ampy)]^{2+}$ (bpy: 2,2'-bipyridine; ampy: 2-(aminomethyl)pyridine) complex were best interpreted in terms of a disproportionation of Ru(III) to Ru(II) and Ru(IV). Also, the stability and reactivity of analogous Os(IV) complexes have been demonstrated.[8] The surprising instability of the $Ru(sar)^{3+}$ ion in acidic aqueous solution,[4] unique so far among saturated Ru(III) hexaamine complexes, prompted an investigation into the factors governing its reactivity. Results of this mechanistic study are presented, and the applicability of a recently proposed model[2] for the dehydrogenation of amines is examined.

In the course of this study, an unusual hydration phenomenon was observed for an imine group coordinated to Ru(II). Observations on this phenomenon are included since we believe that there is a common aspect for both the dehydrogenation of the amine and the hydration of the imine. Furthermore, products of successive oxidations of the $Ru(sar)^{2+}$ complex are analyzed, and the prospects for further modification of the encapsulating ligand are discussed.

Experimental Section

Materials. Deionized (for syntheses) and doubly distilled (for electrochemical and kinetic experiments) water was used. Trifluoromethanesulfonic acid was distilled at reduced pressure before use. $LiCF_3SO_3$ was prepared by neutralizing CF_3SO_3H with LiOH (Merck, p.a.) and dried at 140 °C overnight. $AgCF_3SO_3$ was prepared as described[9] and dried for 6 h in vacuo. Ethanol was dried over 4Å molecular sieves, and acetonitrile (AN) was twice distilled from a small amount of CaH_2 and stored under dry argon in the dark. $n\text{-}Bu_4NCF_3SO_3$ was prepared from $n\text{-}Bu_4NOH$ and CF_3SO_3H and recrystallized twice from dichloromethane/ether (1:10). Stock solutions of Fe_{aq}^{3+} were prepared by dissolution of Fe-powder (Halewood Chem. 99.9999%) in 2 M CF_3SO_3H and oxidation by H_2O_2 (excess decomposed by heating to 50 °C). They were analyzed by atomic absorption spectroscopy. Other products were reagent or analytical grade and used without further purification.

Physical Measurements. UV–vis spectra were recorded with an HP 8450 spectrophotometer. ^1H, ^{13}C, and 2D NMR spectra were recorded with a JEOL FX-200 and a Varian XL200E spectrometer. Electrochemical measurements were performed at 22 °C with the usual three-electrode configuration with a PAR 170 or a BAS 100 electrochemistry system. All the potentials were measured versus Calomel (KCl saturated) or Ag/AgCl (NaCl saturated or acetone/LiCl saturated) but are quoted versus the normal hydrogen electrode NHE (aqueous, by using the couples $(NH_3)_5RuL^{3+/2+}$; L = NH_3, pyridine, nicotinamide, isonicotinamide as reference[10]) or versus $FeCp_2^{+/0}$ (nonaqueous). Glassy carbon (GC) was used as a working electrode and Pt as a counter electrode. Controlled potential coulometry, using an AMEL 551 coulostat and an AMEL 731 digital integrator, was carried out in a commercial PAR cell (50 mL) or a homebuilt small cell (3–10-mL capacity) at a Pt gauze working electrode.

Kinetic experiments were performed with a Gibbs–Durrum D-110 stopped flow reactor equipped with a D-131 photometric log amplifier and a Biomation 805 wave-form recorder. The disproportionation of $Ru(sar)^{3+}$ was followed, after the oxidation of $Ru(sar)^{2+}$ by a suitable oxidant, at different wavelengths by observing the appearance or disappearance of participating species. Oxidants used were Fe_{aq}^{3+}, $(NH_3)_5RuNCCH_3^{3+}$, and $Ni(tacn)_2^{3+}$ (tacn: 1,4,7-triazacyclononane). Particular precautions were taken to exclude all oxygen from the reaction due to the sensitivity of $Ru(sar)^{2+}$ to this reagent. Solutions were flushed with wet argon for 15 min before dissolving known amounts of $[Ru(sar)](CF_3SO_3)_2$ and the oxidant and then evacuated for 1 min to remove the argon. The reservoir syringes were kept in a continuously flushed N_2 atmosphere, and a piece of amalgamated zinc was added to the $Ru(sar)^{2+}$ solution. With these precautions the rates were reproducible to ±10%. An average of 4–6 experiments were performed for a particular reaction condition. Under the conditions chosen all the absorbance time responses were either first (eq 1) or second order (eq 2). The order of the reaction

$$A(t) = A(\infty) + (A(0) - A(\infty)) \exp(-k_{obsd}t) \quad (1)$$

$$A(t) = A(\infty) + (A(0) - A(\infty))/(1 + k'_{obsd}t) \quad (2)^{11}$$

was tested by varying the initial concentrations of the reactants. All calculations were performed on a VAX 11/750 computer by using standard least-squares routines. Buffers used in the kinetic experiments were citric acid/LiOH (pH: 2.8–3.6) and 2,6-dimethylpyridine-3-sulfonic acid/LiOH (pH: 4.1–5.5). The pH was measured with a glass electrode calibrated with hydrogen-phthalate/phthalate, $H_2PO_4^-/HPO_4^{2-}$ and borax buffers. All the experiments (and pH measurements) were performed at 25.0 ± 0.2 °C; after adjustment with $LiCF_3SO_3$ all the solutions were 0.10 M in ionic strength unless indicated otherwise.

Syntheses. All the syntheses and handling of O_2-sensitive compounds were carried out in an atmosphere of purified argon employing Schlenk techniques. $(NH_3)_5RuAN^{3+}$ was prepared as reported[12] and precipitated by addition of $LiCF_3SO_3$. Anal. Calcd (found) for $[(NH_3)_5RuNCCH_3](CF_3SO_3)_3 \cdot 2H_2O$: C, 8.45 (8.4); H, 3.12 (2.8); N, 11.82 (11.3); S_1 13.53 (13.2); F, 24.07 (23.2). $[Ni(tacn)_2](ClO_4)_3$ was synthesized as reported[13] except that Ce^{4+} instead of Co_{aq}^{3+} was used to oxidize $Ni(tacn)_2^{2+}$. Anal. Calcd (found) for $[Ni(C_6H_{15}N_3)_2](ClO_4)_3 \cdot H_2O$: C, 22.75 (22.8); H, 5.09 (5.0); N, 13.27 (13.3); Cl, 16.79 (16.6).

$[Ru(DMF)_6](X)_2$ (X: CF_3SO_3, tos (= toluene-4-sulfonate)). $[Ru(H_2O)_6](X)_2$[14] (7.5 mmol) was added to 50 mL of *N,N'*-dimethylformamide (DMF) which previously had been saturated with argon. The pink-red solution was stirred, and 7.4 g (50 mmol) of O_2-free triethyl orthoformate were added. The tightly stoppered flask was left for 18 h in the dark at room temperature. The solution was then reduced in volume by vacuum distillation (bath temperature ≤ 35 °C), DMF being frozen out in a liquid nitrogen trap. When the volume was about 20 mL, a red-orange product formed. The distillation was continued to almost dryness. The reaction mixture was cooled in an ice bath, an equal amount of diethyl ether was added, and the mixture was vigorously stirred. The product was subsequently filtered off on a P3 frit, well pressed with a glass stopper, and washed with 50 mL of diethyl ether. It was quickly transferred to a glass tube and dried in vacuo in the dark for 2 h. After that the product was a *dry* powder of an orange red ($CF_3SO_3^-$-salt) or light yellow-brown (tos^--salt) color. Yield: ≥80%. Anal. Calcd (found) for $[Ru(C_3H_7NO)_6](CF_3SO_3)_2$: C, 28.67 (29.0); H, 5.05 (5.4); N, 10.03 (10.3); S, 7.65 (7.6); F, 13.61 (13.4).

Note. The product was stored under argon at ≤−20 °C; the dry product can be handled in air for short periods without deterioration.

$[Ru(sar)](X)_2$ (X: CF_3SO_3, tos). $[Ru(DMF)_6](CF_3SO_3)_2$ (1.26 g, 1.5 mmol) or $[Ru(DMF)_6](tos)_2$ (1.32 g) was added in portions at room temperature over a period of 30 min to 10 mL of O_2-free dry ethanol containing 1.7 mmol of sar[3] (0.48 g). Stirring was continued in the dark

(4) Bernhard, P.; Sargeson, A. M. *J. Chem. Soc., Chem. Commun.* **1985**, 1516.
(5) Rudd, De F. P.; Taube, H. *Inorg. Chem.* **1971**, *10*, 1543.
(6) (a) Moyer, B. A.; Meyer, T. J. *Inorg. Chem.* **1981**, *20*, 436. (b) Takeuchi, K. J.; Thompson, M. S.; Pipes, D. W.; Meyer, T. J. *Inorg. Chem.* **1984**, *23*, 1845.
(7) (a) Thompson, M. S.; De Govanni, W. F.; Moyer, B. A.; Meyer, T. J. *J. Org. Chem.* **1984**, *49*, 4972. (b) Meyer, T. J. *J. Electrochem. Soc.* **1984**, 131, 221C and references therein.
(8) (a) Dwyer, F. P.; Hogarth, J. W. *J. Am. Chem. Soc.* **1953**, *75*, 1008; **1955**, *77*, 6152. (b) Lay, P. A.; Sargeson, A. M.; Skelton, B. W.; White, A. H. *Ibid.* **1982**, *104*, 6161.
(9) Jackson, W. G.; Lawrance, G. A.; Lay, P. A.; Sargeson, A. M. *Aust. J. Chem.* **1982**, *35*, 1561.
(10) Brown, G. B.; Krentzien, H. G.; Abe, M.; Taube, H. *Inorg. Chem.* **1979**, *18*, 3374.
(11) For second-order reactions in order for eq 2 to apply, t has to be known accurately (on the time scale of the experiment). Since our reactions were fairly slow, this was not a serious problem. It was found best to carry out the experiments quite speedily in order to minimize the effects of O_2 contamination and/or light sensitivity of the $Ru(sar)^{2+}$ solutions.
(12) Clarke, R. E.; Ford, P. C. *Inorg. Chem.* **1970**, *9*, 227.

(under argon) for 1 h after which the color of the solution had changed from red to yellow-green. The temperature was then slowly raised to reflux (under a blanket of dry argon) and maintained at that level for 12 h. The yellow-orange solution was allowed to cool to room temperature whereupon in some instances, when using the $CF_3SO_3^-$ salt, precipitation of the product occurred. Complete crystallization was achieved by prolonged cooling at −10 °C in an ice/NaCl mixture. The cold reaction mixture was filtered under argon through a P3 Schlenk frit, and the yellow product was then washed with 2 × 50 mL of ether and dried in vacuo. It was recrystallized as the $CF_3SO_3^-$ salt by dissolving it in 10 mL of warm (O_2-free) water, adding 2 mL of 4 M CF_3SO_3H, and cooling to 0 °C. The pale yellow product was isolated on a glass frit, washed with 2 × 20 mL of ether, and dried in vacuo in the dark for 1 h. Yield: 30–70%. Anal. Calcd (found) for $[Ru(C_{14}H_{32}H_6)](CF_3SO_3)_2 \cdot H_2O$: C, 27.39 (27.8); H, 4.88 (4.7); N, 11.98 (12.0); S, 9.14 (9.2); F, 16.24 (16.2).

Note. $[Ru(DMF)_6](X)_2$ should be freshly prepared and not "aged" (brown color). $[Ru(sar)](CF_3SO_3)_2$ was stored under argon in the dark, but it can be handled in air for short periods without problems. Its solutions are very O_2 (and UV-light) sensitive.

$[Ru(sar)](CF_3SO_3)_3$. This compound was obtained by oxidation of $[Ru(sar)](CF_3SO_3)_2$ under anhydrous conditions. The starting material was first recrystallized from dry O_2-free acetonitrile and dried in vacuo for 3 h.

Method (a). $[Ru(sar)](CF_3SO_3)_2$ (0.15 g) was added to 7 mL of 0.2 M n-$Bu_4NCF_3SO_3$/acetonitrile and oxidized at a constant potential of 0.60 V versus Ag/AgCl until the current had dropped to ≤1% of its initial value ($n = 1.0 \pm 0.05$). The volume of the pale yellow solution was reduced to 2 mL by a stream of dry argon and the product, after precipitation with 2 mL of CH_2Cl_2, was isolated on a P3 frit. It was dissolved in acetonitrile to give a saturated solution. Hexagonally shaped crystals were obtained by slowly cooling the solution to −20 °C and were isolated on a filter paper.

Method (b). $[Ru(sar)](CF_3SO_3)_2$ (0.14 g) was added to 2 mL of acetonitrile. Dry $AgCF_3SO_3$ (0.21 mmol, 0.054 g) was added to the stirred solution. This caused an immediate precipitate of Ag metal which was centrifuged off, and the clear pale yellow supernatant solution was evaporated until precipitation occurred. The product was redissolved by gentle heating (≤30 °C), and the solution was cooled to −20 °C to produce the crystalline product which was isolated as described above. Yield: 50–70%. Anal. Calcd (found) for $[Ru(C_{14}H_{32}N_6)](CF_3SO_3)_3$: C, 24.52 (24.8); H, 3.87 (3.85); N, 10.09 (10.2); S, 11.55 (11.4); F, 20.53 (20.8).

Note. Method (b) gave better results. The crystals were stored in a dry atmosphere; in the presence of moisture they decay irreversibly to a yellow powder.

$[Ru(imsar)](CF_3SO_3)_2$. $[Ru(sar)](CF_3SO_3)_2$ (0.48 g) was added to 10 mL of O_2-free 0.4 M CF_3SO_3H in a small electrochemical cell. The product remained largely undissolved and was oxidized, while stirring, at a constant potential of +0.29 V (NHE), until the current had dropped to <1% of its initial value and a clear yellow-green solution had formed. Integration of the current indicated a $2e^-$ oxidation ($n = 2.0 \pm 0.1$). The volume was reduced under argon (by freezing out water into a liquid N_2 trap) to almost dryness and then cooled to −10 °C to produce very fine voluminous needles of a pale yellow product which was isolated on a P3 frit, washed with ether, and dried in vacuo. Yield: ~70%. The extremely soluble product (A) was stored under argon in the dark. It analyzed approximately as $[Ru(C_{14}H_{30}N_6)](CF_3SO_3)_2 \cdot CF_3SO_3H \cdot H_2O$. Calcd (found): C, 23.97 (23.2); H, 3.91 (3.7); N, 9.87 (9.3); S, 11.29 (10.2); F, 20.08 (19.0).

Product A was dissolved in a minimum of water to produce an acidic solution. Upon adjusting the pH to ~7 with Li_2CO_3 a deep yellow product precipitated which was isolated on a frit, washed with ether, dried in vacuo, and stored under argon in the dark. It was converted back to A in strongly acidic conditions. Anal. Calcd (found) for $[Ru(C_{14}H_{30}N_6)](CF_3SO_3)_2$: C, 28.19 (27.4); H, 4.44 (4.4); N, 12.33 (11.9).

$[Ru(hexaimsar)](PF_6)_2$. $[Ru(sar)](CF_3SO_3)_2$ (0.273 g) was added to 5 mL of O_2-free water to give a saturated solution. The solution was vigorously stirred, and 1.23 g (4.8 mmol) of $AgCF_3SO_3$ were added at once to produce immediate precipitation of Ag metal. The color of the solution changed to red-orange and then yellow and, after stirring overnight under argon, to olive green. NH_4PF_6 (0.4 g) was added to the filtered solution producing immediate precipitation of a brown-green product which was recrystallized from water. Yield: 85%. Anal. Calcd (found) for $[Ru(C_{14}H_{20}N_6)](PF_6)_2$: C, 25.35 (25.5); H, 3.04 (3.0); N, 12.67 (12.7).

Results and Discussion

Synthetic Aspects. The complex $Ru(DMF)_6^{2+}$ has proved to be a useful synthetic reagent and has already been used successfully with other ligand systems.[15] Oxidation by Ag^+ in DMF led to the yellow $Ru(DMF)_6^{3+}$ complex which was isolated as the $CF_3SO_3^-$ salt.[16] Rate constants for the DMF exchange in DMF-d_7 are $2 \cdot 10^{-4}$ and $1.4 \cdot 10^{-6}$ s^{-1} for the Ru(II) and Ru(III) ions, respectively,[17] at 25 °C. A comprehensive kinetic and structural characterization of this system as well as a direct route from the common "$RuCl_3 \cdot 3H_2O$" starting material would be of interest. The yield in the $Ru(sar)^{2+}$ synthesis varied between 30% and 70% due to the particular sensitivity of this ion (and of intermediates) toward traces of oxidants; the quality of the $[Ru(DMF)_6](X)_2$ material seemed to be the most important factor as the yield was particularly poor when an "aged" product was used.

The $Ru^{II}sar^{2+}$ ion oxidized readily to the Ru(III) complex, but this then spontaneously disproportionated to the $Ru^{II}sar^{2+}$ and the $Ru^{II}imsar^{2+}$ complex (**2**). However, treatment of the $Ru^{II}sar^{2+}$

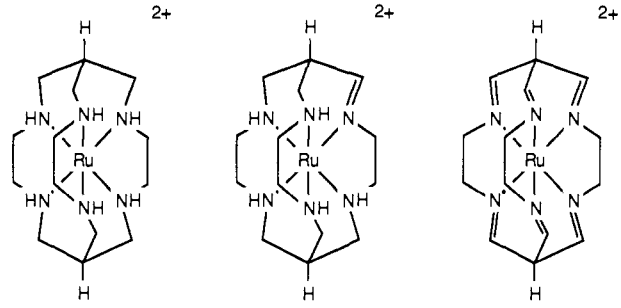

with 2 equiv of Ag^+ gave the $Ru^{II}imsar^{2+}$ ion essentially quantitatively. Further addition of Ag^+ gave isomers of the diimine and then the trimine complexes finally yielding the hexaimine cage complex of Ru(II) (**3**). The isomers of the intermediate imines have not been explored thoroughly at this point, but the oxidation with Ag^+ can be controlled, at least, to give mixtures of the diimine isomers and separately the triimine isomers. Aspects of this oxidation will be referred to later in the paper.

Reactivity of $Ru(imsar)^{2+}$ in Acid. The $Ru^{II}imsar^{2+}$ complex was isolated in two different forms from acidic and neutral solution, respectively, and the constitution of the two forms needs to be established. The ^1H NMR spectra of both compounds (A, B) are shown in Figure 1 (upper part). Complex A exhibits a broad singlet at 6 ppm, whereas for complex B a doublet is found at 8.2 ppm ($J = 5$ Hz). For both complexes fourteen ^{13}C signals were found, indicating a complete loss of symmetry upon oxidation of $Ru(sar)^{2+}$. Thirteen of these signals were between −5 and −30 ppm (versus 1,4-dioxane). The ^{13}C signal of the oxidized carbon site was found at +23 ppm (A) and +96 ppm (B).[18]

The (reversible) transition from B to A is also seen in the absorption spectrum (Figure 1, lower part): When titrating a solution of (B) with CF_3SO_3H, the intense absorption band at 390 nm (for B) disappears in acidic solution. A least-squares fit of the molar absorptivity ϵ as a function of pH (eq 3)

$$\epsilon_{390} = \frac{1}{1 + [H^+]/K_H}(\epsilon(B) + \epsilon(A)[H^+]/K_H) \qquad (3)$$

(13) McAuley, A.; Norman, P. R.; Olubuyide, O. *Inorg. Chem.* **1984**, *23*, 1938.

(14) Bernhard, P.; Bürgi, H. B.; Hauser, J.; Lehmann, H.; Ludi, A. *Inorg. Chem.* **1982**, *21*, 3936.

(15) Keene, F. R., personal communication.

(16) Anal. Calcd (found) for $[Ru(C_3H_7NO)_6](CF_3SO_3)_3$: C, 25.56 (25.5); H, 4.29 (4.4); N, 8.52 (8.3); S, 9.75 (9.4); F, 17.33 (17.0).

(17) Bernhard, P., unpublished observations.

(18) It could unambiguously be shown by 2D NMR techniques that the oxidized site was next to a cage cap.

with the parameters $\epsilon(A)$, $\epsilon(B)$, and K_H gave

$$\epsilon(A) = 300 \pm 100\ M^{-1}\ cm^{-1}$$
$$\epsilon(B) = 4300 \pm 200\ M^{-1}\ cm^{-1}$$
$$K_H = (3.2 \pm 0.5)\cdot 10^{-3}\ M \qquad (pK_H = 2.5 \pm 0.1)$$

(μ = 1.0 M ($LiCF_3SO_3$, CF_3SO_3H), T = 25.0 ± 0.2 °C)

(The pK_H shifted to ~2 for μ = 0.10 M). On the basis of these data compound B is readily identified as structure B in Scheme I. The chemical shifts of the imine carbon and proton are very similar to those found in other Ru(II) imine complexes.[1e,2] The ^1H–^1H coupling constant of the imine proton with the adjacent cage cap proton indicates coplanarity, and the intensity of the absorption band at 390 nm implies charge-transfer character (MLCT) similar to that found for $(NH_3)_5Ru(py)^{2+}$ (λ_{max} (ϵ_{max}) = 406 nm (8000 M^{-1} cm^{-1})[19]). For complex A, a carbinolamine structure is proposed (Scheme I). The chemical shifts of the α-carbon and proton are similar to those found in analogous Co(III)–carbinolamine complexes.[20,21] The small coupling of the α-proton with the cage cap proton indicates that the coplanarity has been lost,[22] and the loss of an intense absorption band indicates that the imine group is no longer present.

The hydration of a coordinated imine group in acidic solution is surprising, and we do not know of other examples in the literature. Coordinated carbinolamine groups are usually obtained in basic conditions by nucleophilic attack at the α-carbon of an imine group.[20,21] No indication of such a process could be found here up to pH 12.

The rate of imine hydration (k_H) was measured after rapid mixing of an aqueous solution of the imine complex (B) with an appropriate acidic solution by following the disappearance of the charge-transfer band at 390 nm. The rates (Table I) were found to be approximately independant of the acid concentration. The implication for the mechanism is that the protonation of the imine complex is fast, followed by a rate-determining addition of a water molecule to the imine group. Thermodynamics requires that the carbinolamine complex (A) be protonated with an apparent dissociation constant (denoted pK_H) of 2.5. Hydration alone could not account for the acid dependence of the equilibrium. A crucial point, therefore, is the site of protonation. Since the rate of hydration is orders of magnitude faster than any reported substitution reactions on Ru(II), a rapid Ru(II)–N bond-breaking process (with subsequent protonation of the amine) can be discounted. Protonation of the C=N double bond is possible but this would lead in the end to a protonated hydroxyl group which does not seem feasible. Such groups usually have pK_a values < 0. Another possibility is protonation at the metal center, and there are good arguments for that path in this instance. The acid-catalyzed substitution of ammonia[23a] on $Ru(NH_3)_6^{2+}$ and substitution reactions[23b] with $(NH_3)_5Rupy^{2+}$ have been interpreted in terms of a protonation of the electron rich Ru(II) metal center leading to a pseudo Ru(IV) hydride species. We will discuss the significance and consequences of such an interpretation later (structure 5 in Scheme III). Unfortunately, our attempts to grow suitable crystals for diffraction studies of the protonated compound (A) have not been successful yet. Location of the proton would probably require neutron diffraction data, but vibrational or ^1H NMR spectroscopy may give less direct evidence to support the suggestion.

Disproportionation of Ru(sar)$^{3+}$ and Related Reactions; Outer-Sphere Oxidation of Ru(sar)$^{2+}$. $Ru(sar)^{3+}$ was generated rapidly by an outer-sphere oxidation (eq 4), and the subsequent slower disproportionation of $Ru(sar)^{3+}$ followed (eq 5). Rate constants (k_1) have been measured for a variety of oxidants.[24]

$$Ru(sar)^{2+} + ox \xrightarrow{k_1} Ru(sar)^{3+} + red \qquad (4)$$

$$2Ru(sar)^{3+} \xrightarrow{k_2} Ru(sar)^{2+} + Ru(imsar)^{2+} + 2H^+ \qquad (5)$$

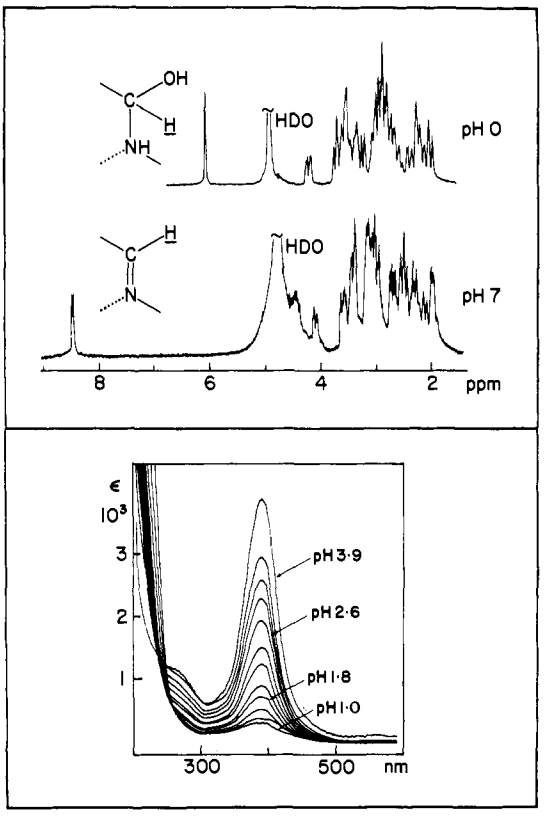

Figure 1. Upper part: 200 MHz ^1H NMR spectrum of $Ru(imsar)^{2+}$ in ~1 M DCl (A, carbinolamine form) and in D_2O (B, imine form); lower part: ϵ_{390} [M^{-1} cm^{-1}] for $Ru(imsar)^{2+}$ as a function of pH.

Scheme I

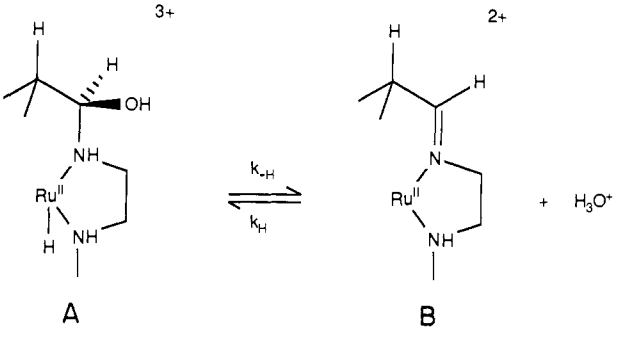

Table I. Rate Constants for Imine → Carbinolamine Hydration[a] for $Ru(imsar)^{2+}$ (T = 25.0 ± 0.2 °C)

pH	k_H (s^{-1})	[CF_3SO_3H] (M)	[$LiCF_3SO_3$] (M)
0.30	212 ± 14	0.50	0.50
0.82	247 ± 18	0.15	0.85
1.30	308 ± 21	0.05	0.95

[a] [$Ru(imsar)^{2+}$] ~ 6–8.10^{-4} M.

Table II. Rate Constants k_1 for Oxidation of $Ru(sar)^{2+}$

oxidant	k_{12} (M^{-1} s^{-1})	μ (M)	ref
Fe_{aq}^{3+}	(7.2 ± 0.6)·10^4	0.10	24
$(NH_3)_5RuNCCH_3^{3+}$	~2.10^6	0.10	25a
$Ni(tacn)_2^{3+}$	~3.10^8	0.10	25b
$Ru(sar)^{3+}$	1.2·10^{5a}	0.10	24

[a] Self-exchange rate, derived from cross-reactions.

(19) Gaunder, H.; Taube, H. *Inorg. Chem.* **1970**, *9*, 2627.
(20) Gainsford, A. R.; Pitzer, R. D.; Sargeson, A. M.; Whimp, P. O. *J. Am. Chem. Soc.* **1981**, *103*, 792.
(21) McCarthy, M. G. Ph.D. thesis, Australian National University, 1984.
(22) The ^1H–^1H coupling constant in the saturated $Ru(sar)^{2+}$ between the α-protons and the cage cap is very small (see Figure 1 in ref 4) J ~ 1.5 Hz.
(23) (a) Ford, P. C.; Kuempel, J. R.; Taube, H. *Inorg. Chem.* **1968**, *7*, 1976. (b) Shepherd, R. E.; Taube, H. *Inorg. Chem.* **1973**, *12*, 1392.

Table III. Rate Constants for Disproportionation of $Ru(sar)^{3+}$ at 25 (±0.2) °C and μ = 0.1 M

	ox	$[ox]_0$[a] (10^{-4} M)	$[Ru(sar)^{2+}]_0$[a] (10^{-4} M)	[buffer][a] (10^{-2} M)	pH	k'_{obsd} (s^{-1})	k_2[b] (10^3 M^{-1} s^{-1})
1	Fe^{3+}_{aq}	3.42	4.86		2.30	3.46 ± 0.26	5.0 ± 0.4
2	Fe^{3+}_{aq}	1.95	4.86		2.30	2.08 ± 0.16	5.3 ± 0.4
3	Fe^{3+}_{aq}	0.98	4.86		2.30	1.00 ± 0.06	5.2 ± 0.3
4	Fe^{3+}_{aq}	0.49	4.86		2.30	0.48 ± 0.02	4.9 ± 0.1
5	Fe^{3+}_{aq}	0.98	4.78		1.70	0.21 ± 0.04	1.1 ± 0.2
6	Fe^{3+}_{aq}	0.98	5.10		1.00	0.0218 ± 0.0014	0.111 ± 0.007
7	$(NH_3)_5RuAN^{3+}$	0.81	5.00		2.30	0.80 ± 0.04	5.0 ± 0.2
8[c]	$(NH_3)_5RuAN^{3+}$	0.94	5.00	1.00[d]	4.85	280 ± 36	$(1.5 \pm 0.2)10^3$
9	$(NH_3)_5RuAN^{3+}$	1.05	5.00	1.00[d]	4.15	68 ± 8	$(3.2 \pm 0.4)10^2$
10	$(NH_3)_5RuAN^{3+}$	0.95	4.90	1.00[e]	3.56	9.0 ± 0.4	47 ± 2
11	$(NH_3)_5RuAN^{3+}$	0.87	4.90	1.00[e]	2.92	3.9 ± 0.2	22 ± 2
12	Fe^{3+}_{aq}	0.49	2.25		2.30	0.57 ± 0.02	5.8 ± 0.2
13	Fe^{3+}_{aq}	0.98	16.1		2.30	0.52 ± 0.02	2.6 ± 0.2
14	Fe^{3+}_{aq}	0.147	0.485		2.30	0.20 ± 0.02	6.8 ± 0.7
15	Fe^{3+}_{aq}	0.98	41.2		2.30	0.236 ± 0.022	1.2 ± 0.1
16	$Ni(tacn)_2^{3+}$	1.17	4.84		2.30	1.14 ± 0.06	4.9 ± 0.6
17	$Ni(tacn)_2^{3+}$	0.93	42.6		3.00	0.38 ± 0.02	2.0 ± 0.1

[a] Concentrations after mixing. [b] $k_2 = k'_{obsd}/2[Ru(sar)^{3+}]_0 = k'_{obsd}/2[ox]_0$. [c] Above pH 4.85 deviation from second order. [d] 2,6-Dimethylpyridine-3-sulfonic acid/LiOH. [e] Citric acid/LiOH.

Scheme II

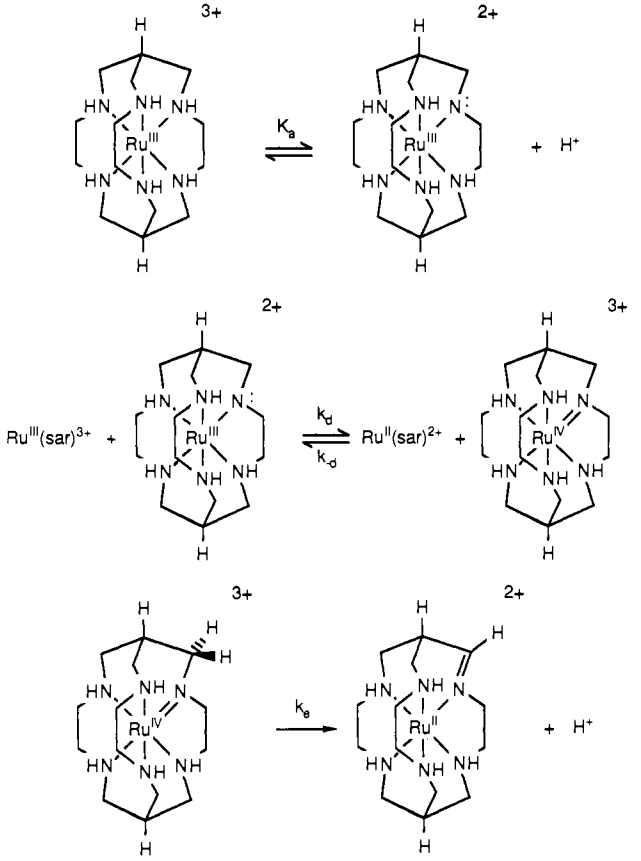

Scheme III

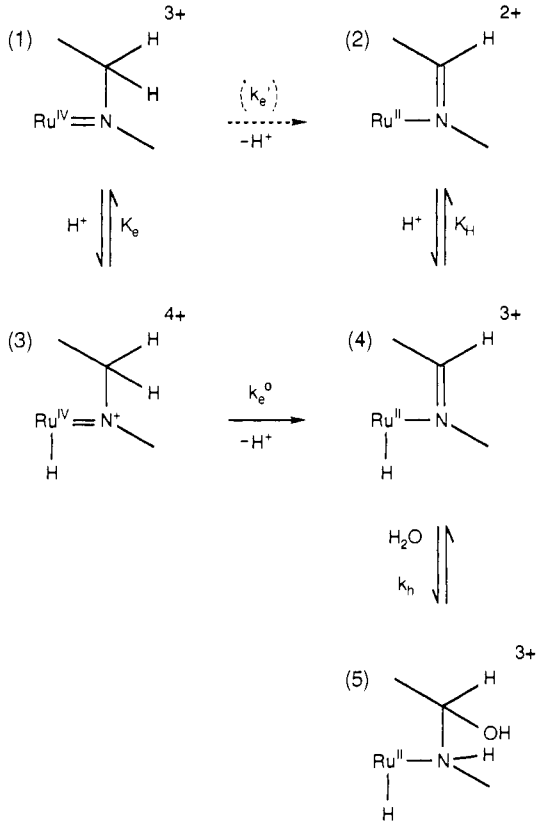

Those for the oxidants used in this study are given in Table II, either measured or estimated from the self-exchange rate constants. Two types of experimental conditions were chosen. In the first series of experiments, $Ru(sar)^{2+}$ was typically in 5-fold excess over the oxidant. In the second series, the oxidant was in exactly 2-fold excess over $Ru(sar)^{2+}$ in which case, due to the remaining equivalent of oxidant, reaction 6 had to be taken into account.

$$Ru(sar)^{3+} + ox(+red) \xrightarrow{k_{ox}} Ru(imsar)^{2+} + red(+red) \quad (6)$$

For the first case (pure disproportionation), k'_{obsd} in eq 2, describing the disappearance of $Ru(sar)^{3+}$, is identified as $2k_2[Ru(sar)^{3+}]_0$. For the second case k'_{obsd} is identified as (k_2 + k_{ox})$[Ru(sar)^{3+}]_0$. ($[Ru(sar)^{3+}]_0$ is the concentration of $Ru(sar)^{3+}$ after the first fast oxidation (eq 4) of $Ru(sar)^{2+}$). Preliminary stoichiometric experiments with the oxidants used showed that under both conditions $Ru(imsar)^{2+}$ was the only ultimate product, i.e., that no polyimine species were produced in observable amounts.

Reaction Order; Acid Dependence; [Ru(sar)$^{2+}$] Dependence. The reaction was followed at 390 nm where $Ru(sar)^{2+}$ and $Ru(sar)^{3+}$ have negligible absorptivity compared to $Ru(imsar)^{2+}$, the appearance of which exhibited a perfect second-order behavior. The absorbance time curves fitted eq 2 closely. Concentrations and rate constants k'_{obsd} and k_2 are given in Table III. Reactions 1–4 illustrate the second-order nature of the process (variation of $[ox]_0 \leq [Ru(sar)^{2+}]_0$); reactions 3, 7, and 16 illustrate the independence of k_2 upon the nature of the oxidant. Plots of log k_2 versus pH (3, 5–11, 16) and versus -log $[Ru(sar)^{2+}]_{av}$[27] (3, 7, 12–16) are

(24) Bernhard, P.; Sargeson, A. M. *Inorg. Chem.* **1987**, *26*, 4122.

shown in Figure 2. The rate constant k_2 is seen to be inverse in $[H^+]$, whereas its dependence upon the Ru(II) concentration is more complicated. At high concentrations of [Ru(II)], k_2 approaches an inverse dependence on $[Ru(sar)^{2+}]_{av}$, but it reaches a limiting value at low concentrations of Ru(II). This behavior indicates a steady-state situation and a combination of all these findings leads to an observed rate law (eq 7) for $Ru(imsar)^{2+}$ formation. From a least-squares fit of the rate constants k_2 to

$$\frac{d[Ru(imsar)^{2+}]}{dt} = \frac{k^\circ_2[Ru(sar)^{3+}]^2}{(1 + K'[Ru(sar)^{2+}]_{av})[H^+]} \quad (7)$$

eq 7 the values $k^\circ_2 = 37 \pm 1\ s^{-1}$ and $K' = (1.21 \pm 0.07)\ 10^3\ M^{-1}$ (at pH = 2.30) were obtained. Note that the term $K'[Ru(sar)^{2+}]_{av}$ is relatively small for the conditions under which the pH dependence was studied. This may have obscured a dependence of K' upon $[H^+]$, and this point will be discussed later, together with reaction 17 in Table III.

Interpretation of the Rate Law. A proposed model[12] for the dehydrogenation of amines, applied to our system, is shown in Scheme II. The disproportionation step involves the reaction between a nondeprotonated and a deprotonated Ru(III) complex to give Ru(II) and Ru(IV). The last is converted, by an intramolecular two-electron transfer and loss of a carbon proton, into the final $Ru^{II}(imsar)^{2+}$ complex. The application of the steady-state approximation for Ru(IV) in the scheme leads to the differential rate law for $Ru(imsar)^{2+}$ formation (eq 8).

$$\frac{d[Ru(imsar)^{2+}]}{dt} = \frac{k_e k_d K_a[H^+][Ru(sar)^{3+}]^2}{(k_e + k_{-d}[Ru(sar)^{2+}])(K_a + [H^+])^2} \quad (8)$$

With the assumption $K_a \ll [H^+]$, the rate law simplifies to eq 9

$$\frac{d[Ru(imsar)^{2+}]}{dt} = \frac{k_e k_d K_a[Ru(sar)^{3+}]^2}{(k_e + k_{-d}[Ru(sar)^{2+}])[H^+]} \quad (9)$$

which is of the same form as our experimentally established rate law (eq 7) and by comparison we obtain (eq 10). The conclusion

$$k^\circ_2 = k_d K_a = 37 \pm 1\ s^{-1} \quad (10a)$$

$$K'(pH = 2.3) = k_{-d}/k_e = (1.21 \pm 0.07) \times 10^3\ M^{-1} \quad (10b)$$

from eq 10a is that the pK_a for $Ru(sar)^{3+}$ has to be *orders of magnitude* lower than that for $Ru(NH_3)_6^{3+}$ (12.4),[28] otherwise the value of k_d becomes larger than the diffusion-controlled limit ($k_{diff} \sim 10^{10}\ M^{-1}\ s^{-1}$ for metal complexes of this size and charge). Even so it appears that the assumption of $K_a \ll [H^+]$ is justified for the conditions used.

Characterization of the Ru(IV) Intermediate. A series of experiments was carried out with a 2-fold excess of oxidant as outlined in the Experimental Section. Also, the measurements were performed in the absence of the buffer to eliminate any possible influence on k_e from this source. The purpose of this study was to accelerate, by the path given in eq 6, the formation of Ru(IV) to the extent that the last step (k_e) would become rate-determining (cf. Scheme II). $Ni(tacn)_2^{3+}$ was used as the rapid oxidant for this purpose (cf. Table II). Under these conditions the rate of absorbance increase at 390 nm (appearance of $Ru^{II}imsar^{2+}$) indeed became first order and therefore independent of the initial concentrations of the reactants. Even more significantly, an intense transient absorption (λ_{max} = 445 nm) was observed which decayed at the same rate as that which increased at 390 nm.

A typical absorbance time curve is shown in Figure 3A together with the absorption spectrum of the transient species (Figure 3B) obtained by varying the wavelength of observation plus an appropriate correction for the overlap with the $Ru(imsar)^{2+}$ spectrum. All the experimental conditions and the rate constants k_e, obtained from first-order least-squares fits, are given in Table IV. There is good agreement between the values of k_e obtained at 390 nm ($Ru(imsar)^{2+}$ appearance) and 450 nm (transient disappearance), and the rate constants are independent of the initial concentration of the reactants (reactions 18 and 19).

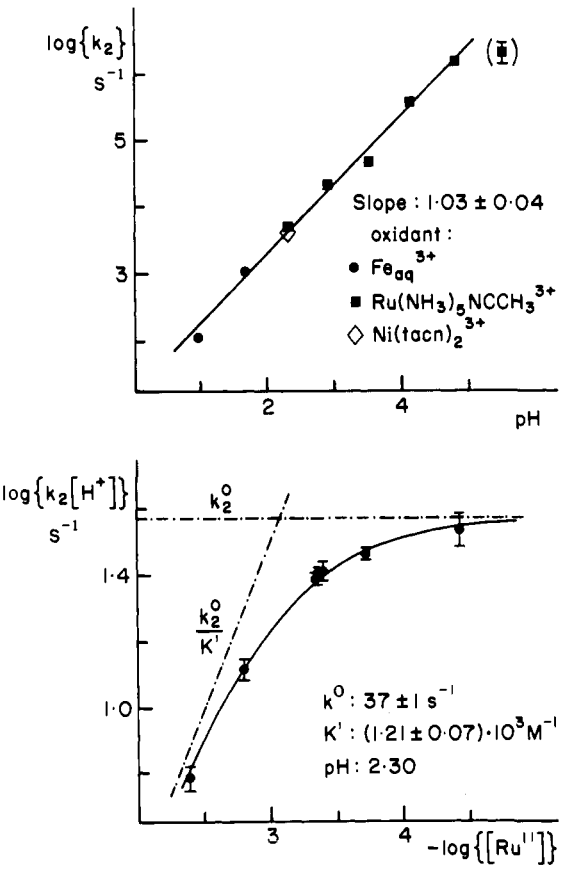

Figure 2. Dependence of the rate constant k_2 (eq 5) for the disproportionation of $Ru(sar)^{3+}$ upon $[H^+]$ and $[Ru(sar)^{2+}]$.

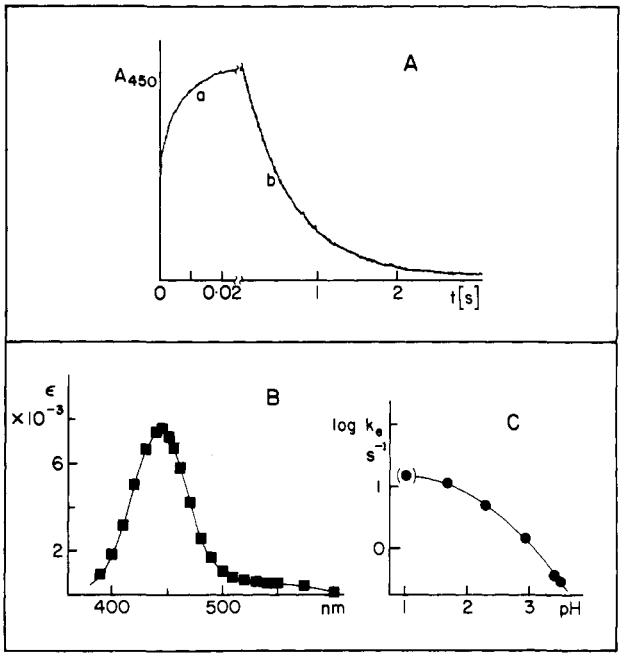

Figure 3. A: Transient absorption observed at 450 nm, ascribed to the deprotonated $Ru^{IV}(sar\text{-}H^+)^{3+}$ complex, in reaction 20 (Table IV). B: Absorption spectrum for the Ru(IV) complex. C: Acid dependence of the $Ru^{IV} \rightarrow Ru^{II}$imine conversion ($k_e$ in Scheme II).

(25) (a) Estimated with the self-exchange rate for $(NH_3)_5RuL^{3+/2+}$ (L:py, nlc, isn);[10] attempts to measure the rate directly were unsuccessful (too fast for the small optical density change). (b) Estimated with the self-exchange rate for $Ni(tacn)_2^{3+/2+}$.[26] The rate was too fast to be measured.

(26) McAuley, A.; Norman, P. R.; Olubuyide, O. *J. Chem. Soc. D* **1984**, 1501.

(27) $[Ru(sar)^{2+}]_{av} = [Ru(II)]_o - 0.5[ox]_o$.

(28) Navon, G.; Waysbort, D. *J. Chem. Soc., Chem. Commun.* **1971**, 1410.

Table IV. Rate Constants k_e for the $Ru^{IV}(sar\text{-}H^+)^{3+} \rightarrow Ru^{II}(imsar)^{2+}$ Conversion in Scheme II at 25 (±0.2) °C and μ = 0.1 M

	$[Ni(tacn)_2^{3+}]_0$[a] (10^{-4} M)	$[Ru(sar)^{2+}]_0$[a] (10^{-4} M)	pH	k_e (s^{-1})	λ_{obsd} (nm)
18	6.10	3.06	2.30	4.9 ± 0.1	390
19	2.00	1.01	2.30	5.3 ± 0.1	450
20	2.02	1.00	2.96	1.49 ± 0.06	390
				1.57 ± 0.07	430–480
21	1.00	0.50	3.50	0.30 ± 0.01	450
22	0.98	1.10	3.40	0.37 ± 0.02	390
				0.34 ± 0.01	450
23	6.05	3.05	1.70	11.9 ± 0.3	450
24	6.65	3.39	1.02	~15	450
		$[Ru(imsar)^{2+}]_0$[a]			
25	2.13	1.05	2.85	1.82 ± 0.05	450[b]
		["$Ru(diimsar)^{2+n}$"]$_0$[a]			
26	2.06	1.01	2.80	1.77 ± 0.06	450[c]

[a] Concentrations after mixing. [b] λ_{max} for $Ru^{IV}(imsar\text{-}H^+)^{3+}$: 440 nm. [c] λ_{max} for "$Ru^{IV}(diimsar\text{-}H^+)^{3+n}$": 430 nm.

As to the nature of this transient species, there can be little doubt that it is a deprotonated Ru(IV) complex by analogy with known Os(IV) chemistry.[8] The intense absorption band at 445 nm (ϵ_{max} = 7800 ± 300 M^{-1} cm^{-1}) can be assigned to a charge transfer from the N lone pair of electrons into the t_{2g} orbital of Ru(IV), but this description is probably over simplistic since the lone pair is strongly delocalized into the metal d-orbitals. The intensity of the band indicates that the interaction is even greater than that for the inverse type of backbonding[29] in $Ru(imsar)^{2+}$. Surprisingly, we could not find any other well characterized examples of Ru(IV) compounds (with saturated N donors) exhibiting such intense absorption bands in the literature. However, a "red color" is reported[5] for the disproportionation of $(NH_3)_5Rupy^{3+}$, with λ_{max} = 524 nm (arsenate buffer, pH 8.3) and 558 nm (carbonate buffer, pH 9.6). In the numerical analysis of Keene et al.,[2] ϵ(Ru(IV)) was floated as a parameter, and values of 400–1000 M^{-1} cm^{-1} (λ = 436 nm, 471 nm) were deduced for the Ru(IV)–aminatomethylpyridine complex. Ru(IV)-oxo complexes show little absorption above 400 nm,[6] but all these complexes contain unsaturated ligands (bipyridine or terpyridine) and are therefore not directly comparable to the present system. Of more relevance, possibly, is the 402-nm absorption band of $Ru(NH_3)_6^{3+}$ at high pH which has been ascribed to the presence of $(NH_3)_5RuNH_2^{2+}$ ($pK_a \sim 12.4$).[28] Although there were some unexplained features in the medium dependence of this system,[30] disproportionation of Ru(III) was not considered at the time. It could be relevant in which case the pK_a deduced[30] is not valid.

Reactions 25 and 26 show that Ru(IV) intermediates were also observed in the disproportionation of $Ru(imsar)^{3+}$ and "$Ru(diimsar)^{3+n}$" (mixture of two isomers) and that they have similar half-lives.

It is evident from Table IV and Figure 3C that k_e has a surprising dependence upon the pH: it appears to *increase* with increasing acidity. Between pH 3.50 and 2.30, k_e is roughly proportional to $[H^+]$, whereas it seems to approach a limiting rate at lower pH values.[31] By implication the Ru(IV) complex has to be protonated in order to assist the loss of a proton on the α-carbon.[1] It can be shown that the Ru(IV) complex is singly but not doubly deprotonated by returning to the rate law for the disproportionation of Ru(III) (eq 9 and 10). Since, k_e has now been found to be acid dependent, the ratio K' ($= k_{-d}/k_e$) is expected to be acid dependent also, unless the Ru(IV) complex is doubly deprotonated in which case the ratio $k'_{-d}[H^+]/k'_e[H^+]$ would be unchanged. To examine this point, we carried out reaction 17 (Table III) at pH 3.00 with a large excess of $Ru(sar)^{2+}$ to make the term $K'[Ru(sar)^{2+}]$ in eq 7 large. No significant absorption was observed at 450 nm under these conditions, and the absorbance increase at 390 nm was second order. Introducing the experimental value of k_2 into eq 7 and using the known value of k°_2 gives $K'(pH = 3.00) = 4.11 \cdot 10^3$ M^{-1}. The ratio (eq 11a) is to be compared with the independently measured ratio in eq 11b (reactions 18–20, Table IV). The close agreement between

$$\frac{K'(pH = 3.0)}{K'(pH = 2.3)} = \frac{k_{-d}/k_e(pH = 3.0)}{k_{-d}/k_e(pH = 2.3)} = 3.4 \qquad (11a)$$

$$\frac{k_e(pH = 2.3)}{k_e(pH = 3.0)} = 3.3 \qquad (11b)$$

the two ratios shows that the back-reaction (k_{-d}) is acid independent and, therefore, that the Ru(IV) complex is only singly deprotonated under these conditions.

These data further imply that the buffers used for reactions 8–11 (Table III) must have a considerable influence on the rate of decay of the Ru(IV) complex. The rate of disproportionation is sufficiently fast in reactions 8–10 in order for the final step to become rate determining (by comparison of k'_{obsd} in Table III and k_e in Table IV). However, the rate of increase in the $Ru(imsar)^{2+}$ concentration was second order implying that the intermediate Ru(IV) species reacts rapidly with the buffer(s) (concentration: 10^{-2} M). Presumably, the base accelerates the deprotonation of the α-carbon. The dependence of the rate upon the nature (and concentration) of the various buffers was not investigated since this aspect cannot be rate determining under conditions which are accessible.

Thermodynamic and Kinetic Implications. By using the experimental parameters in eq 10 and the independently measured values of k_e we calculate the value of k_{-d} (eq 12).

$$k_{-d} = K'(pH = 2.3) \cdot k_e(pH = 2.3) = 6.17 \times 10^3 \ M^{-1} \ s^{-1}$$

$$= K'(pH = 3.0) \cdot k_e(pH = 3.0) = 6.29 \times 10^3 \ M^{-1} \ s^{-1} \qquad (12)$$

We adopt $k_{-d} = 6.2 \times 10^3$ M^{-1} s^{-1}. The equilibrium constant for the process 13a

$$\underset{(III)}{Ru(sar)^{3+}} + \underset{(III)}{Ru(sar)^{3+}} \underset{k_{-d}}{\overset{k^\circ_2}{\rightleftharpoons}} \underset{(II)}{Ru(sar)^{2+}} + \underset{(IV)}{Ru(sar\text{-}H)^{3+}} + H^+ \qquad (13a)$$

is given by eq 13b

$$\frac{k^\circ_2}{k_{-d}} = \frac{k_d K_a}{k_{-d}} = 5.9 \times 10^{-3} \ M \qquad (13b)$$

Since the reduction potential for the $Ru(sar)^{3+/2+}$ couple is known (0.29 V versus NHE)[4] E'(IV/III) for the other half reaction is given by eq 14.

$$E'(IV/III) = 0.29 - 0.059 \log (0.0059) + 0.059 \log [H^+]$$

$$= 0.42 + 0.059 \log [H^+] \ V \qquad (14)$$

Accordingly, the potential for the $Ru(sar\text{-}H^+)^{3+}/Ru(sar)^{2+}$ couple, E'(IV/II), is obtained (eq 15).

$$E'(IV/II) = \frac{E'(IV/III) + E'(III/II)}{2} \qquad (15a)$$

$$= 0.355 + \frac{0.059}{2} \log [H^+] \ V \qquad (15b)$$

It follows from E'(III/II) and E'(IV/III) that the $2e^-$ oxidation of $Ru(sar)^{2+}$ becomes thermodynamically favored over the $1e^-$ oxidation above pH = 2.2 (eq 16). This is precisely reflected

$$pH = \frac{2(0.355 - 0.29)}{0.059} = 2.2 \qquad (16)$$

in the electrochemical response of the system[17] which can be summarized as follows: at pH ≤ 2.0 the potential was independent of pH (E'(III/II) = 0.29 V), and the current corresponded to a $1e^-$ process provided the disproportionation (eq 7) was not important on the time scale of the electrochemical technique.[41] At pH ≥ 2.5 the potential shifted with increasing pH to negative

(29) Chatt, J.; Duncanson, L. A. *J. Chem. Soc.* **1953**, 2939.
(30) Armor, J. N. *J. Inorg. Nucl. Chem.* **1973**, *35*, 2067.
(31) The precision of the value of k_e at pH = 1 is affected by the fact that the buildup rate for Ru(IV), which is inverse in acid ($k_{Ni}K_A/[H^+]$), is no longer fast compared to k_e; therefore the maximum concentration of Ru(IV) reaches only 5% of $[Ru(sar)^{2+}]_0$. At pH = 3.50 however it is 98%.

values, and the current corresponded to a $2e^-$ process. Because of this thermodynamic property of the system a determination of the pK_a for the $Ru(sar)^{3+}$ complex by electrochemical techniques was not possible. Nevertheless, some further related properties can be derived to estimate a range for the pK_a.

Application of the Marcus cross-relation[32] to the disproportionation step (Scheme II) leads to eq 17

$$k_{11}(\text{Ru(sar-H}^+)^{3+/2+}) = \frac{k^\circ_2 k_{-d}}{K_a k_{22}(\text{Ru(sar)}^{3+/2+})} \quad (17)$$

where k_{11} and $k_{22}(Ru^{3+/2+})$ are the self-exchange rate constants for the relevant couples. Accordingly, we obtain the reduction potential for the deprotonated couple, eq 18.

$$E'(\text{Ru(sar-H}^+)^{3+/2+}) = E'(\text{Ru(sar)}^{3+/2+}) - 0.059\left(\log \frac{k^\circ_2}{k_{-d}K_a}\right)[\text{V}] \quad (18)$$

Introduction of all the known experimental rate constants and $E'(Ru(sar)^{3+/2+})$ leads to eq 19 and 20. Even with a negligible

$$k_{11}(\text{Ru(sar-H}^+)^{3+/2+}) = \frac{1.9}{K_a}[\text{M}^{-1}\text{s}^{-1}] \quad (19)$$

$$E'(\text{Ru(sar-H}^+)^{3+/2+}) = 0.29 - 0.059 \log \frac{0.0059}{K_a} \quad (20)$$

inner-sphere reorganization barrier we would expect, for an ion of this size and charge, an upper limit of $\sim 10^6$ M^{-1} s^{-1} for the self-exchange rate constant due to the appreciable solvent reorganization energy.[33] Reasonably, it could be argued that the self-exchange rate constant for the deprotonated Ru(IV/III) couple should be similar to that for $Ru(sar)^{3+/2+}$ (10^5 M^{-1} s^{-1}).[24] This would necessarily imply a pK_a of ~ 5 for $Ru(sar)^{3+}$ and a reduction potential $E'(Ru(sar\text{-}H^+)^{3+/2+}$ of 0.13 V versus NHE. This in turn implies a stabilization of the Ru(IV) oxidation state by deprotonation of ~ 2 V. No $Ru(sar)^{3+}$ oxidation was seen in strongly acidic solution below the solvent limit (1.5 V versus NHE on glassy carbon in 2 M CF_3SO_3H) and in acetonitrile (2 V versus ferrocene on Pt). A comparably large stabilization has been observed for Os(IV).[8]

An extraordinarily low pK_a (5–6) for $Ru(sar)^{3+}$ seems inescapable. The analysis of the $(bpy)_2Ru(ampy)^{3+}$ system yielded a pK_a of 2.5 for the primary amine which was interpreted[2] in terms of the release of some strain in the five-membered ring system upon deprotonation (and the effect of the backbonding with the bpy ligands). For the cage, the strain could play a crucial part in the adjustment of the coordination geometry. A planar configuration at the deprotonated nitrogen atom can be readily achieved by a slight twist at the cage cap. The somewhat related base hydrolysis of Ru(III) amine complexes arising from deprotonation at ammine sites has been found to be very sensitive to the nature of the amine ligands.[34] Although this may be only partly due to a variation in pK_a, proton exchange rates would be more significant, but data for Ru(III) are limited at present. For Co(III) cyclam complexes, variations of several orders of magnitude have been found for the proton exchange rates.[35]

The derived rate law (eq 8) predicts a maximum rate constant of disproportionation at $pH = pK_a$ ($k_d/4$) and a decrease at higher pH. Unfortunately, our attempts to extend the measurements above pH 5 (cf. Figure 2) were unsuccessful due to the lack of a suitable oxidant; $Ni(tacn)_2^{3+}$, which would have been ideal, is much less stable under these conditions. The $OH^\bullet$ radical, which is a powerful oxidant, would achieve the fast oxidation of $Ru(sar)^{2+}$ (eq 21), and a series of pulse radiolysis experiments[36] were conducted with this oxidant. The strategy was unsuccessful in the sense that we could not observe the disproportionation of Ru(III) at such low concentrations ($\sim 10^{-6}$ M), but an interesting observation was made. $Ru(sar)^{2+}$ was found to react with $OH^\bullet$ at a diffusion-controlled rate to form a species which exhibited a high absorptivity between 400 and 500 nm and which was stable on the maximum time scale available to follow the experiment (~ 1 s). Since this instantaneously generated species cannot be the deprotonated Ru(IV) complex, we attributed this absorption to the deprotonated Ru(III) complex, generated by hydrogen atom abstraction at the secondary nitrogen (eq 22) and rapid intramolecular electron transfer (eq 23).

$$\text{Ru}^{II}\text{—N—H} + \text{OH}^\bullet \longrightarrow \text{Ru}^{II}\text{—N}^\bullet + \text{H}_2\text{O} \quad (22)$$

$$\text{Ru}^{II}\text{—N}^\bullet \longrightarrow \text{Ru}^{III}\text{—N:} \quad (23)$$

Under the experimental conditions (pH = 7–8) the Ru(III) complex seems to be stable and not to be rapidly reprotonated; a pK_a of 5–6 could account for that behavior.

Mechanisms of Amine Dehydrogenation and Imine Hydration. There are similarities between the hydration phenomenon in the $Ru(imsar)^{2+}$ complex (Scheme I) and the acid dependence of the intramolecular electron transfer step (k_e, cf. Scheme III). The rate constant, k_e, seems to approach a limiting value in the pH region (<2) where the $Ru(imsar)^{2+}$ becomes fully hydrated indicating that the rate is a composite of an equilibrium and a rate constant (eq 24) with $k^\circ_e \sim 17$ s^{-1} and $K_e \sim 10^{-2}$ M. The value

$$k_e = \frac{k^\circ_e}{1 + K_e/[\text{H}^+]} \quad (24)$$

of pK_e is close to the pK_H (cf. Figure 2, eq 3) of the $Ru(imsar)^{2+}$ complex. The crucial point in both cases is the site of protonation. Because of the observed acid catalysis of substitution reactions[23,37] on hexaamine Ru(II) complexes and the absence of other feasible protonation sites, the most likely site for protonation is a nonbonding orbital on the d^6 Ru(II) metal center. A mechanistic proposal for both processes is shown in Scheme III. Structure **4** is a common intermediate, and step (3) → (4) is expected to be faster than the acid-independent step (1) → (2). Although structure **2** seems to be somewhat questionable, the only alternative possibility (which would lead to the same acid dependence), $Ru(sar)^{4+}$, is very unlikely for thermodynamic reasons ($E'(Ru(sar)^{4+/3+} > 2$ V). It is expected from this scheme that k_e should reach a limiting value at higher pH (k'_e); however, the proton loss on the α-carbon might become inverse in acid as OH^- instead of H_2O becomes the base for deprotonation. It is plausible from the preceding argument that a buffer (~ 0.01 M) substantially increases the rate of either of the irreversible steps (k°_e or k'_e).

The protonation phenomenon is expected to disappear as the Ru(II) oxidation state becomes more stable since H^+ is no longer able to "ionize" Ru(II) to (formally) a "Ru(IV)–hydride" complex. This is indeed observed; only for monoimine or diimine complexes was there an indication of hydration of an imine group in ≤4 M acid. Progressively, π-acceptor ligands reduce the electron density on Ru(II) and therefore the affinity for H^+. Systems in which Ru(II) is greatly stabilized by π-acceptors (like the $(bpy)_2Ru(ampy)^{2+}$ complex) are not expected to exhibit the hydration phenomenon or a direct acid dependence of k_e.

An important consequence of the proposed mechanism is that $Ru(sar)^{2+}$ itself should also exhibit the protonation phenomenon. This point was not thoroughly examined. In all the experiments, $CF_3SO_3^-$ was used as a counterion. The salt which was obtained from 0.1–1.0 M CF_3SO_3H occasionally contained some H_2O which could be removed by drying the compound exhaustively in vacuo. The fact that no $[HRu(sar)](CF_3SO_3)_3$ was obtained

$$\text{Ru(sar)}^{2+} + {}^\bullet\text{OH} \rightarrow \text{Ru(sar)}^{3+} + \text{OH}^- \quad (21)$$

(32) Marcus, R. A. *Ann. Rev. Phys. Chem.* **1964**, *15*, 155.
(33) Sutin, N. *Progr. Inorg. Chem.* **1983**, *30*, 489.
(34) Poon, C. K.; Isabirye, D. A. *J. Chem. Soc. D* **1977**, 2115; **1978**, 740.
(35) Lichtig, J.; Sosa, M. E. *J. Chem. Soc. D* **1984**, 581.
(36) $^\bullet OH$ was generated with a van de Graaf e^- accelerator (AAEC, Lucas Heights, Australia), by the reaction $e_{aq}^- + N_2O + H_2O \rightarrow N_2 + {}^-OH + {}^\bullet OH$.
(37) Taube, H. *Surv. Prog. Chem.* **1973**, *6*, 1 and references therein.

could be due to the insolubility of $[Ru(sar)](CF_3SO_3)_2$ in CF_3SO_3H.

To examine whether the protonation had any effect on the rate of proton exchange in $Ru(sar)^{2+}$, the H/D exchange rate was measured at pH = 1 (0.1 M DCl) and at pH = 7 (D_2O) at 22 °C. The respective rate constants, $1.3 \cdot 10^{-3}$ s^{-1} (0.1 M DCl) and $5 \cdot 10^{-3}$ s^{-1} (D_2O), do not indicate a large effect by H^+ but they do have implications. Normally, in amine complexes these exchanges are inverse in $[H^+]$ so the value at pH 1 does imply an acid catalysis. More experiments need to be done over the whole pH range however to define the pH profile, but these experiments are difficult to do because traces of $Ru(sar)^{3+}$ complicate the issue. One further point which arises from these studies is that there is no proton exchange at the methylene groups in any oxidation state nor in the imine oxidation product.

The acid- and base-catalyzed proton losses described for the Ru(IV) intermediate are akin to those observed in organic carbonyl chemistry. The high bond order for the Ru(IV)=N< bond labilizes the protons on the adjacent methylene groups toward removal by a base. These bonds will be substantially shorter than the remaining Ru–N single bonds (~0.2–0.3 Å).[1e,8b] Clearly, the donation of the lone pair of electrons from the N center to the d^4-Ru(IV) ion is at a profound level which greatly influences the properties of the organic moiety and gives the Ru(IV) ion a much greater basicity than in its absence. Under these conditions, Ru(IV) appears to approach Ru(II) in fact. It follows that protonation of the Ru(IV) ion also leads to labilization of the proton on the methylene group via a tautomeric effect even in the absence of bases apart from water.

Further Oxidation of $Ru(imsar)^{2+}$. In Figure 4 a cyclic voltammogram of $Ru(sar)^{2+}$ (A) in 0.1 M CF_3SO_3H at a scan rate of 0.02 V s^{-1} is shown. Six equally spaced (~0.15 V) oxidation waves are evident plus another well separated. We interpret the six waves as oxidations of $Ru(sar)^{2+}$ and then the successively formed Ru(II) mono-, di-, tri-, tetra-, and pentaimine complexes (in the case of di-, tri-, and tetraimines presumably mixtures of several isomers). The products are formed rapidly on the time scale of the (slow) scan, but whether acid catalysis of the $Ru^{IV}(imine)_x \rightarrow Ru^{II}(imine)_{x+1}$ conversion (cf. Figure 3C for the case of $Ru^{IV}sar$) occurs in all cases or whether the rate constants k'_e in Scheme III are inherently greater for higher oxidized complexes we are not able to tell. The similarity of the rate constant k_e for the $Ru(imsar)^{2+}$ and the "$Ru(diimsar)^{2+}$" complexes to that for $Ru(sar)^{2+}$ at pH = 3 implies that the overall behavior is similar.

As a consequence of this interpretation the separate wave at +1.15 V should be assigned to the oxidation of the $Ru(hexaimsar)^{2+}$ (**3**) complex. This was indeed confirmed by using isolated and characterized $[Ru(hexaimsar)](PF_6)_2$, as discussed below. The CV of $Ru(imsar)^{2+}$ (B) under the same conditions is identical except for the first wave. The $Ru(imsar)^{2+}$ complex was then electrooxidized at 0.42 V (NHE). After $2e^-$ were consumed and the current had dropped to ca. 8% of its initial value, the electrolysis was stopped. A product was isolated which was a mixture of two major diimine complexes (established by 2D NMR techniques). One of the complexes had two imine groups in the same cap producing a chemical shift of the apical cap proton which was roughly twice the shift observed in $Ru(imsar)^{2+}$, whereas for the other complex the imine groups were located in different caps. Further oxidation of this mixture increased the complexity of species present, but the presence of one complex with three imine groups in the same cap was established. Separation of the various complexes which were still O_2-sensitive was not achieved on Sephadex SPC 25 ion exchange resin, but there was no indication of α,β-diimine oxidation in any of the products. Ru(II) polyimine complexes were also obtained after stoichiometric oxidations with Ag^+, but the product distribution was very dependent upon the conditions under which Ag^+ was added.

In acetonitrile, $Ru(sar)^{2+}$, $Ru(imsar)^{2+}$, and the mixture of $Ru(diimsar)^{2+}$ complexes (denoted "$Ru(diimsar)^{2+}$" exhibited reversible behavior with reduction potentials −0.18, −0.03 and +0.11 V (versus $FeCp_2^{+/0}$), respectively, confirming the 0.14–0.15 V in stabilization of Ru(II) by each imine group. Roughly the same stabilization energy had been observed for coordination of pyridine[38] in place of NH_3.

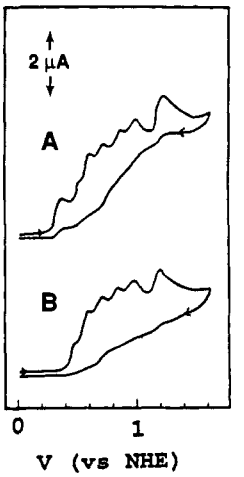

Figure 4. Cyclic voltammograms of $Ru(sar)^{2+}$ (A) and $Ru(imsar)^{2+}$ (B) in 0.1 M CF_3SO_3H on a glassy carbon electrode (d = 0.6 cm) using a scan rate of 0.02 V s^{-1} at 22 °C. $[Ru^{II}] = 10^{-3}$ M.

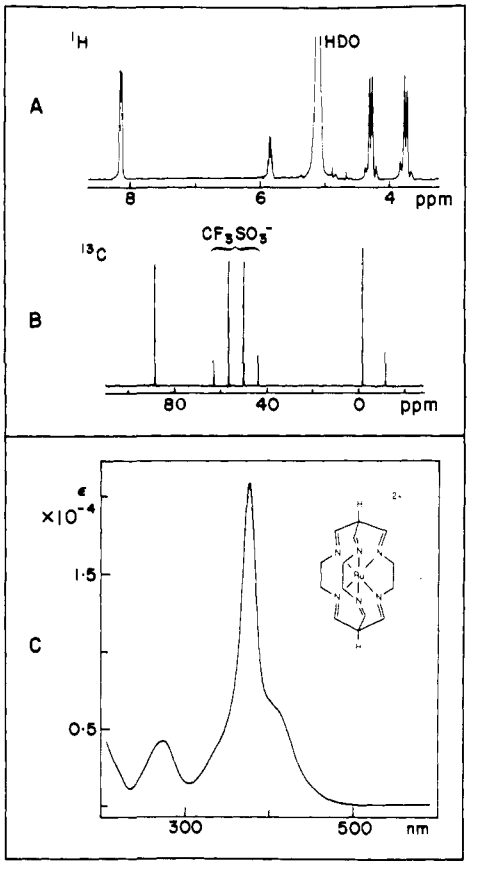

Figure 5. Upper part: 200 MHz ^1H and 50 MHz ^{13}C NMR spectra of $Ru(hexaimsar)^{2+}$ in D_2O (reaction mixture). Lower part: absorption spectrum of $[Ru(hexaimsar)](PF_6)_2$ in H_2O.

A remarkable observation was made when either $Ru(sar)^{2+}$ or $Ru(imsar)^{2+}$ was reacted with respectively 12 and 10 equiv of $AgCF_3SO_3$ in H_2O (D_2O). The ^1H and ^{13}C NMR spectra of the reaction mixture in the D_2O experiment is shown in Figure 5 (A and B) confirming that the conversion to the D_3-$Ru(hexaimsar)^{2+}$ ion **3** was quantitative. The complex was isolated as described in the Experimental Section. Its absorption spectrum is shown in Figure 5C and exhibits several bands, one of which (λ_{max} (ϵ_{max}) = 377 nm (22 000 M^{-1} cm^{-1})) is unusually sharp ($\Delta_{1/2}$ = 1680 cm^{-1}). This is reminiscent of the Soret bands in metal ion porphyrin complexes. Work is in progress to elucidate the electronic structure of this unique complex, which is oxidized at 1.15 V

(versus NHE). The total stabilization is 0.86 V (1.15 ← 0.29 V) for six imine groups (i.e., 0.145 V per imine group), very similar to that for the extensively investigated $Ru(bpy)_3^{2+}$ complex (E' = 1.24 V). The Ru(hexaimsar)$^{2+}$ complex could thus be a prototype for a new series of electrochemically and photochemically interesting Ru complexes.

Conclusions

This study provides another example of the ability of ruthenium(III) to promote dehydrogenation of aliphatic amine complexes via deprotonated Ru(IV) complexes. The direct observation and characterization of these intermediate Ru(IV) complexes is one of the most significant results of our investigation. Also, Ru(hexaimsar)$^{2+}$ is an unprecedented species. There emerge, moreover, interesting differences in reactivity between closely related systems: $Ru(en)_3^{2+}$ can be oxidized to the corresponding α,β-diimine complex by a 4e$^-$ oxidation, but the reactivity of $Ru(en)_3^{3+}$ is orders of magnitude lower than that of $Ru(sar)^{3+}$, and also $Ru(1,4,7\text{-triazacyclononane})_2^{3+}$ is stable on the voltammetric time scale at slow scan rates up to pH = 5.[42] This implies at least six orders of magnitude difference in the second-order disproportionation rate constant even though, in Scheme II, $Ru(tacn)_2^{3+}$ is a slightly better oxidant than $Ru(sar)_3^{3+}$ (0.37 and 0.29 V versus NHE). An important factor in the oxidation is the ease with which a planar configuration about the deprotonated N atom can be achieved. This factor would lower the pK_a and increase the Ru(IV)–N$^-$ bond order which in turn increases the driving force for the disproportionation step (Scheme II). Clearly, $Ru^{IV}(tacn)(tacn\text{-}H^+)^{3+}$ has more difficulty achieving this configuration than the ethanediamine and sarcophagine complexes due to the ligand configurations. However, once an imine group has been introduced into the ethanediamine fragment this will greatly favor a second oxidation in the same fragment due to the conjugation in the five-membered planar ring system. This notion also accommodates the very fast dehydrogenation of the $(bpy)_2Ru(ampy)^{3+}$ complex. Similar observations have been made in Fe systems.[39] Clearly this qualitative picture would have to be substantiated by strain calculations as soon as structural information on the complexes is available.

The assumption of a linear acid dependence of k_e (eq 24) up to pH ~ 6 leads to a lifetime of ~10 min for the deprotonated Ru(IV) complex which should make its isolation possible. However, working on a preparative scale (0.01–0.1 M) produces the same concentration of H$^+$ (which catalyzes the Ru(IV)-aminato → Ru(II)-imine conversion), and buffers cannot be used; therefore, the isolation of the Ru(IV) intermediate may be a difficult task.

It is most interesting to examine the prospect of modifying the Ru(hexaimsar)$^{2+}$ complex. Further oxidation in water presumably leads to the introduction of amides. A more interesting variation would be the reaction with good nucleophiles (e.g., aromatic Grignard reagents or organolithium compounds) to extend the aromatic framework of the ligand. Other strategies would employ different ligands from the outset while applying the same synthetic route. A most interesting example would be the 1,2-diaminocyclohexane cage which might be aromatized via the Ru(III) complex and then further (reversibly) oxidized to an *o*-phenylenediimine fragment.[3] It is well known that such groups, when coordinated to Ru(II), lead to very highly colored species.[40] These could be attractive candidates for pigments. The synthetic routes already worked out point the way for many other developments in the cage chemistry or related areas.

One of the most intriguing facets of this investigation is the regiospecificity of the ligand oxidation which is confined to the cap moieties of the cage despite the fact that conjugation in the ethanediamine fragments would be favored from the organic point of view. Clearly, there is an interplay between the demands of the metal ion and the ligand which can be sensed at the point where the proton is lost from the carbon atom. Each act of H$^+$ loss appears to lead to net oxidation of the ligand. We are currently exploring the relative rates of oxidation of different amines bound to Ru(III) and Fe(III) to see what governs their rate and specificity. It is also apparent that protonation of the metal ion leads to very interesting modulation of the reactivity of bound ligands and this effect is being explored further also.

Acknowledgment. We are grateful to the Microanalytical Service Unit of the ANU for analyses, to the Australian Institute for Nuclear Science and Engineering for assistance with the pulse radiolysis experiments, and to Professor H. B. Bürgi (University of Bern) for helpful discussions. P.B. thanks ANU for a postdoctoral fellowship.

Registry No. 1, 101482-30-8; **2**, 117203-74-4; **3**, 117203-72-2; sar, 64189-50-0; imsar, 117226-37-6; $[Ru(DMF)_6](CF_3SO_3)_2$, 101461-83-0; $[Ru(DMF)_6](tos)_2$, 114378-79-9; $[Ru(H_2O)_6](CF_3SO_3)_2$, 99617-78-4; $[Ru(H_2O)_6](tos)_2$, 15694-44-7; $[Ru(sar)](CF_3SO_3)_3$, 117226-36-5; $AgCF_3SO_3$, 2923-28-6; $[Ru(C_{14}H_{30}N_6)](CF_3SO_3)_2{\cdot}CF_3SO_3H$, 117203-70-0; $[Ru(DMF)_6](CF_3SO_3)_3$, 101461-85-2; Ru(sar-H$^+$)$^{3+}$, 117203-75-5; Ru(sar-H$^+$)$^{2+}$, 117203-76-6; Ru(diimsar)$^{2+}$, 117203-77-7; Ru(triimsar)$^{2+}$, 117203-78-8; $(NH_3)_5RuNCCH_3^{3+}$, 44819-54-7; $Ni(tacn)_2^{3+}$, 86709-81-1.

(38) Creutz, C.; Zwickel, A. M. *Inorg. Chem.* **1971**, *10*, 2395. See, also: *Chelating Agents & Metal Chelates*; Dwyer, F. P., Mellor, D. P. Eds.; Academic Press: New York, 1964; p 269.

(39) Goto, M.; Takeshita, M.; Kanda, N.; Sakai, T.; Goedken, V. *Inorg. Chem.* **1985**, *24*, 582.

(40) Joss, S.; Bürgi, H. B.; Ludi, A. *Inorg. Chem.* **1985**, *24*, 949.

(41) Although the disproportionation given in eq 13a is not favored at pH < 2.2 the reaction is driven by the acid-catalyzed Ru(IV) → Ru^{II}imsar^{2+} conversion (see Table IV).

(42) Bernhard, P.; Sargeson, A. M. *Inorg. Chem.* **1988**, *27*, 2582.